

Using Attractor Dynamics to Generate Decentralized Motion Control of Two Mobile robots Transporting a Long Object in Coordination

Rui Soares¹, Estela Bicho^{2*}

¹ *Escola Superior de Tecnologia e Gestão de Felgueiras, Portugal, soares.rui@mail.telepac.pt*

² *Dep. Electronica Industrial, Universidade do Minho, Portugal, estela.bicho@dei.uminho.pt*

Abstract

Dynamical systems theory is used here as a theoretical language and tool to design a distributed control architecture for a team of two mobile robots that must transport a long object and simultaneously avoid obstacles. In this approach the level of modeling is at the level of behaviors. A “dynamics” of behavior is defined over a state space of behavioral variables (heading direction and path velocity). The environment is also modeled in these terms by representing task constraints as attractors (i.e. asymptotically stable states) or repellers (i.e. unstable states) of behavioral dynamics. For each robot attractors and repellers are combined into a vector field that governs the behavior. The resulting dynamical systems that generate the behavior of the robots may be non-linear. By design the systems are tuned so that the behavioral variables are always very close to one attractor. Thus the behavior of each robot is controlled by a time series of asymptotically stable states. Computer simulations support the validity of our dynamic model architectures.

1 Introduction

The problem of controlling and coordinating several autonomous robots that cooperatively carry a large-size object has received much attention from researchers working on cooperative robotics (e.g.[1,2,3,7,8,13]). The motivation is that such a system of robots is very useful in industrial and civil environments where material handling and transportation tasks are required. There two general approaches for controlling multiple robots transporting an object: (1)- centralized control schemes and (2)-decentralized control schemes. The limited success of (1) is due to communication costs, (2) is better but there is a major difficulty: to control precisely the motion/behavior of each individual robot is very

difficult. From the point of view of a cooperating robot the environment, which consists of the manipulated object, the other robots and the world scenario (static or dynamic), exhibits complex dynamic behavior. The problem is exacerbated when the environment is unknown and no path is given. We address here the problem of controlling and coordinating the movement of two mobile robots that cooperatively perform the task of transporting a long object (e.g. a bar, a ladder) toward a goal destination in a two dimensional environment with obstacles. Particular to our work, we investigate how behavior-based coordinated/cooperative transportation can be generated by non-linear dynamical systems (or more specifically non-linear attractor dynamics). The work is based on the so called Dynamic Approach to Behavior Generation [10,11] which provide a number of useful concepts.

We assume that the robots have no prior knowledge of the environment and we choose a *leader-follower* decentralized motion control strategy. A *leader* robot drives from an initial position to a final target destination. The other robot (i.e. *follower*) takes the *leader* as a reference point, and must steer so as to keep at all times the correct formation (i.e. orientation and distance to the *leader*) that permits it to cooperate with the *leader* in the transportation task and simultaneously avoid any obstacles that may appear (see Figure 1).

The control architecture of each robot is structured in terms of elementary behaviors. The individual behaviors and their integration are generated/modeled by non-linear dynamical system and we use bifurcation theory to make design decisions around points at which a system must switch from one type of solution to another [5]. The benefit is that the mathematical properties associated with the concepts (c.f. Section 3) enable system integration including stability of the overall behavior of the autonomous systems. Simulation results indicate that if the parameter val-

*E. Bicho is the corresponding author

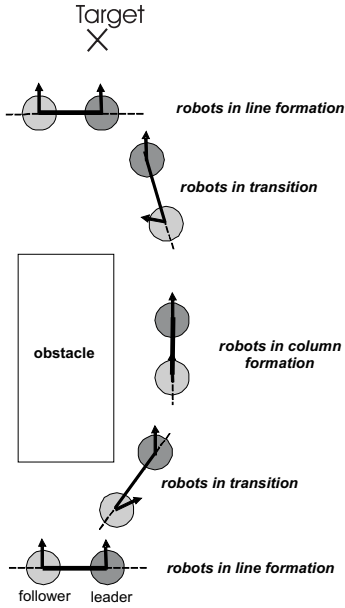


Figure 1: Cooperative object transportation by two robots in an unknown environment. By default the robots must transport the object keeping a line formation. When due to encountered obstacles that is not possible the follower robot must change its direction of navigation appropriately as illustrated.

ues are chosen within certain reasonable ranges, then the overall system works quite well even in narrow cluttered environments.

The rest of the paper is structured as follows: in the next section we present the organization of the robot team and the basic assumptions in this work. In Section 3 we define and describe the behavioral dynamics for each robot in the team. Results obtained from simulation studies are presented in Section 4. The paper ends with Section 5 with a brief discussion, conclusions and an outlook for future work.

2 The team of robots and their tasks

We briefly discuss the organization of the team of mobile robots and we outline the basic assumptions for this work. The simulated robots are based on a physical mobile robot where the motion control architecture presented in Subsection 3.1 has been previously implemented and evaluated [5,6]. Each simulated robot consists of a cylindrical platform with two lateral wheels (see Figure 2).

The control and coordination of the two robots is based on the following ideas: *i)* The behavior of each robot is controlled independently. *ii)* The team's *leader* knows the target position. The task of this robot consists in moving toward the goal while avoid-

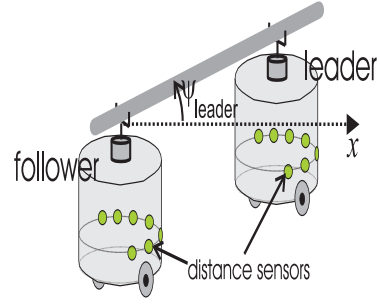


Figure 2: Each robot has seven distance sensors mounted on a ring which is centered on the robot's rotation axis. These are used to measure the distance to obstructions at the directions in which they are pointing in space. The simulated sensors mimic the IR sensors mounted on the physical robot, i.e. they have a distance range of 60 cm and an angular range of 30 deg. The robots are tightly coupled through a rotary and a prismatic free joints as depicted.

ing collisions with encountered obstacles. *iii)* The *follower* must “help” the *leader* to carry the long object from the initial position to the final target destination. This implies that the task constraint of the follower robot consists in steering so as to keep at all times a correct formation (i.e. orientation and distance to the leader). By default the robots must transport the object side by side (i.e. line formation). However, due to the obstacles this might not be possible. When obstructions are encountered by the *follower* it must then drive in “transition” and/or column formation. Once it is possible it must return to the line formation again (Figure 1). *iv)* The *leader* shares with the *follower* only its current path velocity and heading direction. The *follower* does not send any information to the *leader*. Our decision makes the task scenario more challenging for the *follower*. *v)* Each robot has a free rotational joint and a free prismatic joint. These are used to support the object. Additionally, these give important information to the *follower* robot: *a)* From the current angle of the free rotational joint the *follower* knows the direction at which the *leader* robot lies as seen from its current position and with respect to the external reference axis (i.e. ψ_{leader}); *b)* displacements (Δd) measured in the free prismatic joint are used by the *follower* to know its distance to the *leader* ($d = d_{\text{desired}} + \Delta d$). *vi)* The desired distance (d_{desired}) between the two robots is a function of the size of the object to carry and we assume that it can vary maximally ± 10 cm (i.e. $\Delta d_{\text{max}} = \pm 10$) from the desired value.

3 Attractor dynamics for coordinated transportation

We start with a brief review of the basic ideas of the dynamic approach to behavior generation (see e.g. [10,11,5] for more details): (1) *Behavioral variables* are used to describe, quantify and internally represent the state of the robot system with respect to elementary behaviors. For an autonomous mobile robot moving in the plane, the *heading direction*, ϕ ($0 \leq \phi \leq 2\pi$ rad), with respect to an arbitrary but fixed world axis, and *path velocity*, v , are appropriate behavioral variables. (2) Behavior is generated by continuously providing values to these variables, which control the robot's wheels. The time course of each of these variables is obtained from (constant) solutions of dynamical systems. The attractor solutions (asymptotically stable states) dominate these solutions by design. In the present system, the *behavioral dynamics* of heading direction, $\phi_i(t)$, and velocity, $v_i(t)$, ($i = \text{leader, follower}$) are differential equations

$$\dot{\phi}_i = f_i(\phi_i, \text{parameters}) \quad (1)$$

$$\dot{v}_i = g_i(v_i, \text{parameters}). \quad (2)$$

Task constraints define contributions to the vector fields, $f_i(\phi_i, \text{parameters})$ and $g_i(v_i, \text{parameters})$. Each constraint may be modeled either as a repulsive or as an attractive force-let, which are both characterized by three parameters: (a) which value of the behavioral variable is specified? (for example in the case of ϕ_{leader} the specified values might be ψ_{obs} , ψ_{tar} (see Figure 3) (b) how strongly attractive or repulsive the specified value is?; and (c) over which range of values of the behavioral variable a force-let acts? Thus, in isolation, each force-let creates an attractor (asymptotically stable state) or a repeller (unstable state) of the dynamics of the behavioral variables. An attractive force-let serves to attract the system to a desired value of the behavioral variable (e.g. the direction in which a target lies for the heading direction or a desired velocity value for the path velocity). A repulsive force-let is used to avoid the values of the behavioral variable that must be avoided (for example, the directions in which obstacles lie are values that the heading direction must avoid).

The resultant dynamical systems may be nonlinear and have multiple stable states (attractors). By design, parameters are tuned such that the behavioral variables are very close to one attractor of the resultant dynamics most of the time. Thus the behavior of each robot is generated as time series of asymptotically stable states. The fact that only attractor solutions matter can be used to design the layout of attractors and repellers using the qualitative theory of dynamical systems. Qualitative changes in

the behaviour are brought about through bifurcations in the vector fields. Local bifurcation theory helps to design the dynamics such that these qualitative changes are automatically made under the appropriate environmental conditions (e.g. sensory information and shared information among the team of robots).

Next, we built the behavioral dynamics, i.e. we derive the vector fields of Eq. 1 and Eq. 2, for each robot.

3.1 Behavioral dynamics of the leader

A. Attractor dynamics for heading direction.

As is illustrated in Figure 3, the direction, ψ_{tar} , in which a target position lies as seen from the current position of the *leader* robot specifies a desired value for the heading direction. Directions, ψ_{obs} , in which obstacles lie specify values of heading direction that must be avoided.

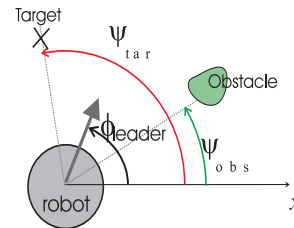


Figure 3: Constraints for the dynamics of ϕ_{leader} are the directions at which obstacles and target lie from the current position of the robot, i.e. directions ψ_{obs} and ψ_{tar} .

If the direction, ψ_{tar} , in which the target lies, with respect to the current position of the robot is known, then a simple dynamical system that generates orientation toward the target direction can be designed that creates an attractor at that direction (see Figure 4):

$$\begin{aligned} \dot{\phi}_{\text{leader}} &= f_{\text{tar}}(\phi_{\text{leader}}) \\ &= -\lambda_{\text{tar}} \sin(\phi_{\text{leader}} - \psi_{\text{tar}}) \end{aligned} \quad (3)$$

When the robot moves it must not collide with obstacles. The directions in which obstructions are detected must therefore be avoided. This can be expressed by a dynamical system that repel from these directions. Each distance sensor ($i = 1, 2, \dots$), mounted on an angle θ_i relative to the forward direction of the robot, contributes with a repulsive force-let (see Figure 5). The complete obstacle avoidance dynamics reads:

$$\dot{\phi}_{\text{leader}} = \sum_i f_{\text{obs},i}(\phi_{\text{leader}}) \quad (4)$$

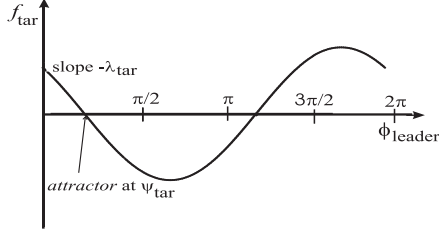


Figure 4: The direction $\phi_{\text{leader}} = \psi_{\text{tar}}$ is a fixed point attractor ($\dot{\phi}_{\text{leader}} = 0$ there with negative slope) with strength λ_{tar} . Because target acquisition is desired from any starting orientation of the robot the range over which this attractor exerts its attractive effect is the entire full circle, i.e. from 0 to 2π rad. As a consequence, there is a repeller at the back, in the direction opposite to that toward the target (i.e. $\psi_{\text{tar}} + \pi$).

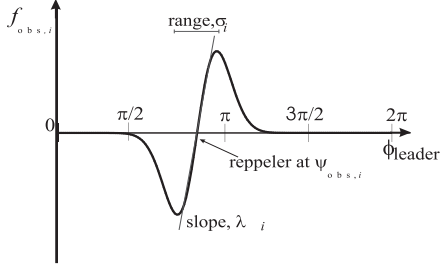


Figure 5: A contribution to the dynamics of heading direction expressing the task constraint “avoid direction of the obstacle” is a force-let with a fixed point repeller (zero with positive slope) at the direction, $\psi_{\text{obs},i}$ at which an obstruction has been detected. Every distance sensor ($i = 1, 2, \dots, 7$) contributes with such a force-let centered on the direction in which the sensor points. By decreasing the slope (λ_i) with increasing measured distance, only nearby surfaces repel strongly. The range of the force-let (σ_i) is limited based on sensor range and on the constraint of passing without contact.

where

$$f_{\text{obs},i} = \lambda_i (\phi_{\text{leader}} - \psi_{\text{obs},i}) \exp \left[-\frac{(\phi_{\text{leader}} - \psi_{\text{obs},i})^2}{2\sigma_i^2} \right] \quad (5)$$

Here $\psi_{\text{obs},i}$ is the direction in the world in which sensor i is pointing. As the heading direction, ϕ_{leader} , is defined relative to the same reference frame, the relevant difference, $\phi_{\text{leader}} - \psi_{\text{obs},i} = -\theta_i$ is actually a constant. This illustrates that the calibration of the robot’s heading direction in the world is irrelevant. The strength of repulsion, λ_i , of each contribution is a decreasing function of the sensed distance:

$$\lambda_i = \beta_1 \exp[-d_i/\beta_2] \quad (6)$$

which depends on two parameters controlling overall strength (β_1) and spatial rate of decay (β_2). The

angular range,

$$\sigma_i = \arctan \left[\tan\left(\frac{\Delta\theta}{2}\right) + \frac{R_{\text{robot}}}{R_{\text{robot}} + d_i} \right] \quad (7)$$

over which the contribution exerts its repulsive effect is adjusted taking both sensor sector, $\Delta\theta$, and the minimal passing distance of the vehicle (at size R_{robot} of the platform) into account (details may be found in [4,5]).

The target contribution and the contributions arising from the detected obstructions all act at the same time. The *leader* heading direction dynamics is thus simply the sum over these:

$$\dot{\phi}_{\text{leader}} = f_{\text{tar}}(\phi_{\text{leader}}) + \sum_{i=1}^7 f_{\text{obs},i}(\phi_{\text{leader}}) + f_{\text{stoch}} \quad (8)$$

More sophisticated control over activation and de-activation of such contributions can be obtained using activation networks [12,13] but is not necessary here. Since some of the force-lets have limited range, this superposition is a non-linear dynamical system, which may have multiple attractors and repellers (typically few). By design the system is tuned so that the heading direction is in a resulting attractor of this dynamics most of the time (c.f. Section 4). The stochastic force, f_{stoch} , guarantees escape from unstable fixed points (repellers). This is important because it might happen that due to a bifurcation in the heading direction dynamics, the attractor (desired value) in which the heading direction was settled becomes a repeller (i.e. an undesired value).

B. Velocity control dynamics. Up to this point we have only addressed the control of the *leaders*’ heading direction. For this robot to move it must have some path velocity, of course. As it moves, sensory information changes and thus attractors (and repellers) shift. The same happens if obstacles or the target move (c.f. Subsection 3.2) in the world. Since the heading direction must be in or near an attractor at all times, for the design principle to work, we must limit the rate of such shifts to permit the robot’s heading direction to track the attractor as it moves and thus stay close to a stable state. This is possible by controlling the robot’s path velocity, v_{leader} , by means of a dynamical system

$$\dot{v}_{\text{leader}} = g_{\text{tar}}(v_{\text{leader}}) + g_{\text{obs}}(v_{\text{leader}}) \quad (9)$$

where each contribution to the vector field is a force-let that erects an attractor at the required velocity, $v_{\text{leader},i}$, with strength, c_i and range σ_v : ($i = \text{tar}, \text{obs}$)

$$g_i = c_i (v_{\text{leader}} - v_{\text{leader},i}) \exp \left[-\frac{(v_{\text{leader}} - v_{\text{leader},i})^2}{2\sigma_v^2} \right]. \quad (10)$$

The strengths, c_{obs} and c_{tar} , are adjusted such that in the presence of strong obstacle contributions the obstacle term dominates while in the absence of such contributions the reverse holds (see [5,6] for details).

C. Hierarchy of relaxation rates. Finally, the following hierarchy of relaxation rates ensures that the heading direction of the leader robot relaxes to the attractor solutions as they change due to varying sensory information and that obstacle avoidance has precedence over target acquisition:

$$\lambda_{\text{tar}} \ll c_{\text{tar}}, \quad \lambda_{\text{obs}} \ll c_{\text{obs}}, \quad \lambda_{\text{tar}} \ll \lambda_{\text{obs}}, \quad (11)$$

The complete behavioral dynamics for the *leader* robot has been implemented and evaluated in detail on a physical mobile robot (see e.g. Chapter 4 in [5]).

3.2 Behavioral dynamics of the *follower*

To control the behavior of the *follower* we use its heading direction, ϕ_{follower} , with respect to an arbitrary external reference frame and its path velocity, v_{follower} .

A. Attractor dynamics for heading direction.

In the absence of sensed obstacles the *follower* helps the *leader* in the transportation task by keeping a line formation as depicted in the top panel of Figure 6.

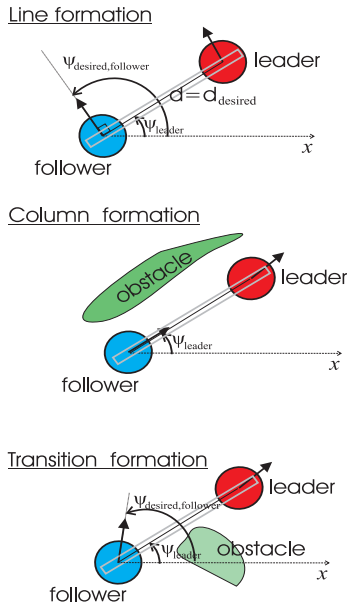


Figure 6: Desired orientations for the follower robot as a function of the required formation configuration.

A behavioral dynamics for the *follower's* heading direction that generates line formation taking the

leader robot as a reference point is

$$\begin{aligned} \dot{\phi}_{\text{follower}} &= f_{\text{line}}(\phi_{\text{follower}}) \\ &= f_{\text{attract}}(\phi_{\text{follower}}) + f_{\text{repel}}(\phi_{\text{follower}}) \end{aligned} \quad (12)$$

where each term defines an attractive force ($i = \text{attract, repel}$)

$$f_i(\phi_{\text{follower}}) = -\lambda_{\text{line}} \lambda_i(d) \sin(\phi_{\text{follower}} - \psi_i) \quad (13)$$

where the first contribution, f_{attract} , erects an attractor at a direction $\psi_{\text{attract}} = \psi_{\text{leader}} + \pi/2 - \Delta\psi$. The strength of this attractor ($\lambda_{\text{line}} \lambda_{\text{attract}}(d)$ with λ_{line} fixed), increases with distance, d , between the two robots:

$$\lambda_{\text{attract}}(d) = 1/(1 + \exp(-(d - d_{\text{desired}})/\mu)). \quad (14)$$

The second contribution, f_{repel} , sets an attractor at a direction pointing away from the *leader*, $\psi_{\text{repel}} (= \psi_{\text{leader}} + \pi/2 + \Delta\psi)$ with a strength ($\lambda_{\text{line}} \lambda_{\text{repel}}(d)$) that decreases with distance, d , between the robots,

$$\lambda_{\text{repel}}(d) = 1 - \lambda_{\text{attract}}(d). \quad (15)$$

Because these two attractive forces are overlapping only one attractor results from their superposition. The direction at which the resulting attractor emerges depends on the distance between the two robots. This is illustrated in Figure 7.

In the presence of a long obstacle or in narrow passages the *follower* must drive behind the *leader* (see middle panel of Figure 6). A simple dynamical system for the *follower's* heading direction that generates navigation in column formation taking the *leader* as a reference point is

$$\begin{aligned} \dot{\phi}_{\text{follower}} &= f_{\text{col}}(\phi_{\text{follower}}) \\ &= -\lambda_{\text{col}} \sin(\phi_{\text{follower}} - \psi_{\text{leader}}) \end{aligned} \quad (16)$$

which erects an attractor for ϕ_{follower} directly at the direction at which the *leader* lies as seen from the current position of the *follower* (i.e. ψ_{leader}).

When moving around an obstacle as illustrated in the bottom panel of Figure 6 the desired value for the *followers's* heading direction is $\psi_{\text{leader}} + \Delta\psi$ if the obstacle is to the right or $\psi_{\text{leader}} - \Delta\psi$ if the obstacle is to the left. An adequate and simple dynamical system that generates the time course of the heading direction of this robot during the “transition formation” reads

$$\begin{aligned} \dot{\phi}_{\text{follower}} &= f_{\text{tran}}(\phi_{\text{follower}}) \\ &= -\lambda_{\text{tran}} \sin(\phi_{\text{follower}} - \psi_{\text{tran}}) \end{aligned} \quad (17)$$

which erects an attractor at $\psi_{\text{tran}} = \psi_{\text{leader}} + \alpha_{\text{obs}} \Delta\psi$ with fixed strength of attraction λ_{tran} . α_{obs} is a function that takes the value -1 if the *follower* detects

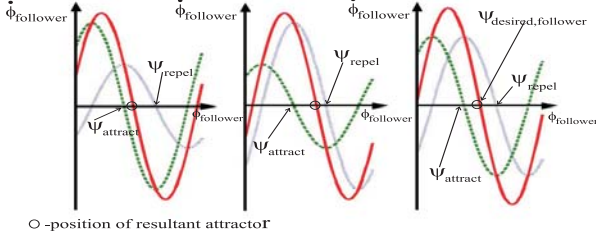


Figure 7: This figure shows the two contributions to the line formation dynamics and their superposition for the three different physical situations. f_{attract} and f_{repel} are depicted by the dotted and dashed thin lines respectively. Their superposition, i.e. f_{line} , is indicated by the bold continuous line. Left: When the distance between the two robots is larger than the desired distance the attractive force erected at direction ψ_{attract} is stronger than the attractive set at direction ψ_{repel} . Their superposition leads to an attractor at a direction still pointing towards the movement direction of the leader robot. Middle: Conversely, when the distance between the two robots is smaller than the desired distance, the reverse holds, i.e. the attractive force set at direction ψ_{attract} is now stronger than the attractive force at direction ψ_{repel} . The resulting line formation dynamics exhibits an attractor at a direction pointing away from leader's direction of movement. Right: When the robots are at the desired distance the two attractive forces have the same strength which leads to a resultant attractor at the orientation parallel to the leader's movement direction, i.e. $\psi_{\text{desired,follower}} = \psi_{\text{leader}} + \pi/2$.

obstructions on its left side or is equal to 1 if obstructions are to the right. In fact, from the sign of the obstacle resulting forces sensed by the *follower*, we can read off, if the obstacle is to the left or to the right of the robot and thus be able to select the correct attractor state for the heading direction of this robot:

$$\alpha_{\text{obs}}(\phi_{\text{follower}}) = \begin{cases} -1 & \text{for } \sum_{i=1}^7 f_{\text{obs},i}(\phi_{\text{follower}}) < 0 \\ 1 & \text{else} \end{cases} \quad (18)$$

where each $f_{\text{obs},i}(\phi_{\text{follower}})$ has the same functional form of Eq. 5, i.e. it is a repulsive force-let that would repel ϕ_{follower} from the directions at which the follower's sensors detect obstructions (if these would be used to generate obstacle avoidance dynamics in this robot in a similar way as for the *leader*).

Finally, the complete behavioral dynamics of the *follower*'s heading direction is governed by:

$$\dot{\phi}_{\text{follower}} = \gamma_{\text{line}} f_{\text{line}}(\phi_{\text{follower}}) + \gamma_{\text{tran}} f_{\text{tran}}(\phi_{\text{follower}}) + \gamma_{\text{col}} f_{\text{col}}(\phi_{\text{follower}}) \quad (19)$$

Where γ_{line} , γ_{tran} and γ_{col} are mutually exclusive activation variables that, depending on the sensorial in-

formation acquired by the distance sensors mounted on the *follower* robot and the current heading direction of the *leader* robot (i.e. $\phi_{\text{leader}}(t)$), determine which component term of the vector field must dominate the dynamics.

In the absence of obstacles the term f_{line} must dominate the vector field, so $\gamma_{\text{line}} = 1, \gamma_{\text{tran}} = 0$ and $\gamma_{\text{col}} = 0$ is required. Conversely, when obstructions are detected and the difference between the direction ψ_{leader} and ϕ_{leader} is larger than 5 deg the robots must drive as depicted in the bottom panel of Figure 6, so the term f_{tran} must dominate the vector field ($\gamma_{\text{line}} = 0, \gamma_{\text{tran}} = 1$ and $\gamma_{\text{col}} = 0$ must hold). Else, if obstructions are detected but the difference between the direction ψ_{leader} and ϕ_{leader} is smaller than 5 deg we want the robots to move in column formation (middle panel of Figure 6), thus $\gamma_{\text{line}} = 0, \gamma_{\text{tran}} = 0$ and $\gamma_{\text{col}} = 1$ is desired.

A function that indicates if obstacle contributions are present is the potential function of the virtual obstacle avoidance dynamics for this robot:

$$U_{\text{obs}}(\phi_{\text{follower}}) = \sum_{i=1}^7 \lambda_{f,i} \sigma_{f,i}^2 \left(\exp \left[-\frac{(\phi_{\text{follower}} - \psi_{f,\text{obs},i})^2}{2\sigma_{f,i}^2} \right] - 1/\sqrt{e} \right) \quad (20)$$

where $\psi_{f,\text{obs},i}$ is the direction in which distance sensor i of the *follower* robot is pointing, $\lambda_{f,i}$ is the magnitude of repulsion from this direction and $\sigma_{f,i}$ is the angular range of repulsion ($\lambda_{f,i}$ and $\sigma_{f,i}$ have the functional form of Eq. 6 and Eq. 7 respectively).

Positive values of this potential function indicate that the *follower*'s heading direction is in a repulsion zone of sufficient strength. Conversely, negative values of the potential indicate that the heading direction is outside the repulsion range or repulsion is very weak. Applying a sigmoidal threshold function to the potential we get a function that ranges from -1 to 1 :

$$\alpha_{\text{pot}}(\phi_{\text{follower}}) = 2 \arctan[c U_{\text{obs}}(\phi_{\text{follower}})]/\pi \quad (21)$$

Also, applying a sigmoidal threshold function to the difference $\text{abs}(\psi_{\text{leader}} - \phi_{\text{leader}}) - 5 \text{deg}$:

$$\alpha_{\Delta} = 2 \arctan[c (\text{abs}(\psi_{\text{leader}} - \phi_{\text{leader}}) - 5 * \pi/180)]/\pi \quad (22)$$

we can finally write the following functions for the activation variables:

$$\gamma_{\text{line}} = 1 - \alpha_{\text{pot}} * (1 + \alpha_{\text{pot}})/2 \quad (23)$$

$$\gamma_{\text{tran}} = \alpha_{\text{pot}} * (1 + \alpha_{\text{pot}}) * (1 + \alpha_{\Delta})/4 \quad (24)$$

$$\gamma_{\text{col}} = \alpha_{\text{pot}} * (1 + \alpha_{\text{pot}}) * (1 - \alpha_{\Delta})/4 \quad (25)$$

At sufficiently sharp sigmoids (c sufficiently large) this leads to the required term in the vector field of the *followers*'s heading direction dynamics.

B. Velocity control dynamics. The path velocity of the *follower* must be controlled so that this robot keeps the desired distance to the *leader* at all times. A necessary condition to help the *leader* to carry the object with success. At each instant in time the *follower*'s required path velocity depends on the path velocity of the *leader* (i.e. $v_{\text{leader}}(t)$), on the constraint to drive at a fixed distance from the *leader*, and accelerations and decelerations must be a function of the current heading direction of the *leader* robot so that the appropriate formation configuration can be maintained during movement. This can be accomplished by controlling the *follower*'s path velocity, v_{follower} , by means of a dynamical system

$$\begin{aligned} \dot{v}_{\text{follower}} = & \gamma_{\text{line}} g_{\text{line}}(v_{\text{follower}}) \\ & + \gamma_{\text{tran}} g_{\text{tran}}(v_{\text{follower}}) + \gamma_{\text{col}} g_{\text{col}}(v_{\text{follower}}) \end{aligned} \quad (26)$$

where each contribution to the vector field is a force-let that erects an attractor at the required velocity, $v_{\text{follower},i}$, with strength, c_i and range σ_v : ($i = \text{line, tran, col}$)

$$g_i = c_i (v_{\text{follower}} - v_{\text{follower},i}) \exp \left[-\frac{(v_{\text{follower}} - v_{\text{follower},i})^2}{2\sigma_v^2} \right] \quad (27)$$

C. Hierarchy of relaxation rates. Finally, the following hierarchy of relaxation rates ensures that the heading direction of the *follower* robot relaxes to the attractor solutions as they change due to varying sensory information and varying information communicated by the *leader*:

$$\lambda_{\text{line}} \ll c_{\text{line}}, \quad \lambda_{\text{tran}} \ll c_{\text{tran}}, \quad \lambda_{\text{col}} \ll c_{\text{col}}, \quad (28)$$

4 Results

The complete dynamic architectures were evaluated in computer simulations. These were generated by a software simulator written in MATLAB. We modeled the robotic platforms, based on the physical prototype in which the dynamic control architecture described in Subsection 3.1 has been previously implemented. In the simulation the robots are represented as triplets (x_j, y_j, ϕ_j) ($j = \text{leader, follower}$), consisting of the corresponding two Cartesian coordinates and the heading direction. Cartesian coordinates are updated by a dead-reckoning rule ($\dot{x}_j = v_j \cos(\phi_j)$, $\dot{y}_j = v_j \sin(\phi_j)$) while heading direction, ϕ_j , and path velocity, v_j , are obtained from the corresponding behavioral dynamics. All dynamical equations are integrated with a forward Euler method with fixed time step, and sensory information is computed once per each cycle. Distance sensors are simulated through an algorithm reminiscent of ray-tracing. The target information is defined by a goal

position in space (i.e. $(x_{\text{tar}}, y_{\text{tar}})$). It is assumed here that the *leader* robot broadcasts its current velocity and heading direction to the *follower*.

A simulation run in a complex scenario which demonstrates several features of the dynamic control architectures is presented in Figure 8. Figure 9 shows the heading direction dynamics for each robot, at the points showed in snapshots A, B and D.

5 Conclusions and future work

We have demonstrated how attractor dynamics can be used to design a distributed dynamic control architecture that enables a team of two robots to carry a long object and simultaneously avoid obstacles. The robots have no prior knowledge of their environment. The behavior is generated by a time series of attractor solutions. Simulation studies have shown that the robots' behavior is stable and that the generated trajectories are smooth. As the sensed world changes the systems change their planning solutions adequately. The work described here imposes of course further research. The complete distributed dynamical architecture must be implemented (and evaluated) in a robot team composed of two physical autonomous robots. Next, we must generalize our approach to larger teams of robots.

Acknowledgments

This project was supported, in part, through grant POSI/SRI/38051/2001 from the portuguese Foundation for Science and Technology (FCT). We also thank Wolfram Erihagen, Sergio Monteiro, Aventino Cardoso and Francisco Mendonca for discussions.

References

- [1] M N Ahmadabadi and E Nakano. A Constraint and Move“ Approach to Distributed Object Manipulation. *IEEE Transactions on Robotics and Automation*, 17(2):157–172, 2001.
- [2] T Arai and J Ota. Dwarf intelligence - A large object carried by seven dwarves. *Robotics and Autonomous Systems*, 21:23–35, 1997.
- [3] Y Asahiro, E C Chang, A Mali, I Suzuki and M Yamashita. A distributed Ladder Transportation Algorithm for Two Robots in a Corridor. *in Proc. IEEE Int. Conf. Robotics and Automation*, 3016–3021, 2001.
- [4] E Bicho and G Schöner. The dynamic approach to autonomous robotics demonstrated on a low-level vehicle platform. *Robotics and Autonomous Systems*, 18:149–155, 1996.
- [5] E Bicho. Dynamic Approach to Behavior-Based Robotics: design, specification, analysis, simulation and implementation. Shaker Verlag, ISBN 3-8265-7462-1, Aachen, 2000.
- [6] E Bicho, P Mallet, and G Schöner. Target representation on an autonomous vehicle with low-level sensors.

The International Journal of Robotics Research, Vol. 19, No.5, May 2000, pp.424-447.

- [7] L Chaimowicz, T Sugar, V Kumar and M Campos. An Architecture for Tightly Coupled Multi-Robot Cooperation. *in Proc. IEEE Int. Conf. Robotics and Automation*, 2292-2297, 2001.
- [8] K Kosuge, H Takeda, Y Hirata. Decentralized Motion Control of Two tracked Mobile Robots Transporting a Single Object in Coordination Based on Function Allocation Concept. *in Aro Workshop 2000 on Intelligent Systems, Australian National University, Canberra, Australia, Dec. 8-9, 2000*.
- [9] E W Large, H I Christensen, and R Bajcy. Scaling the dynamic approach to path planning and control: Competition among behavioral constraints. *International Journal of Robotics Research*, 18(1):37-58, 1999.
- [10] G Schöner and M Dose. A dynamical systems approach to task-level system integration used to plan and control autonomous vehicle motion. *Robotics and Autonomous Systems*, 10:253-267, 1992.
- [11] G Schöner, M Dose, and C Engels. Dynamics of behavior: Theory and applications for autonomous robot architectures. *Robotics and Autonomous Systems*, 16:213-245, 1995.
- [12] A Steinhage. *Dynamical Systems for the Generation of Navigation Behavior*. Shaker Verlag, Aachen, 1998.
- [13] M Uchiyama and P Dauchez. A symmetric hybrid position/force control scheme for the coordination of two robots. *in Proc. IEEE Int. Conf. Robotics and Automation*, 350-355, 1988.

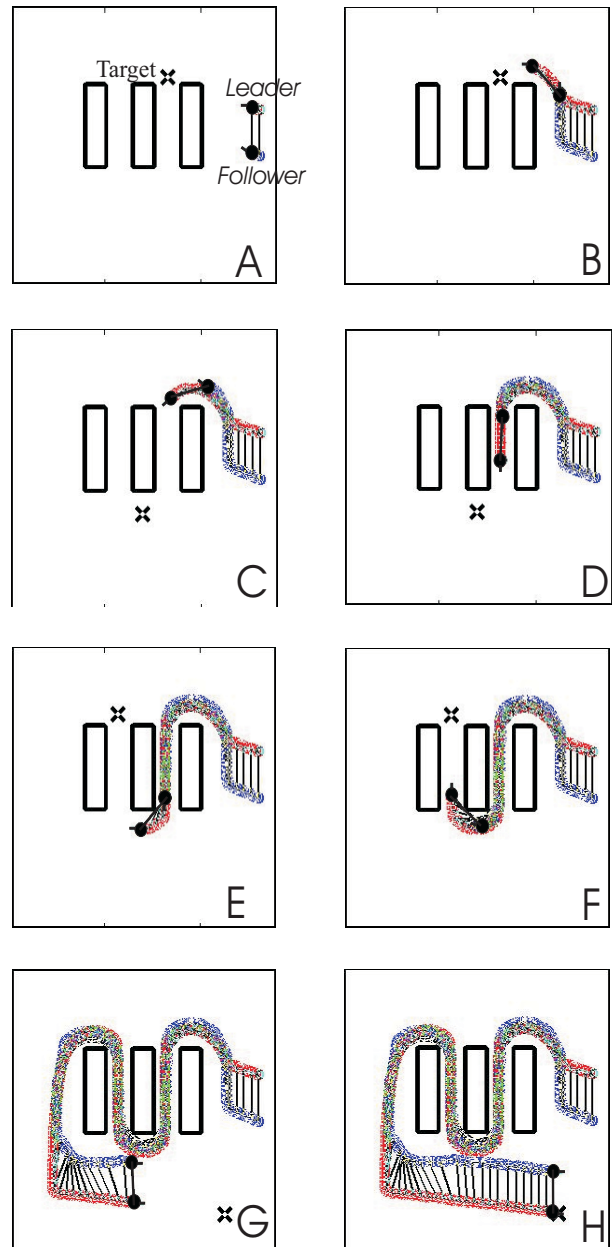


Figure 8: Snapshots of a simulation run of the complete system. The target is indicated by a cross. The robots are represented by black circles with a line indicating their heading direction. Initially, the robots are placed as indicated in Panel A. The leader moves toward the target location and simultaneously avoids the obstacle (Panel B). The follower starts by steering so as to keep a line formation with the leader (Panel A). When it detects the obstacle it turns right and steers so that it follows the leader and simultaneously avoids collisions with the obstacle (Panel B). Once the target is reached, the target is shifted to the position indicated in Panel C, and so on. The leader enters into the narrow passage. During the movement through this narrow passage the follower keeps a column formation with the leader (Panels C- E). Again, once the target is reached, the target is shifted again, this time to position indicated in Panel H. The leader always moves toward the target and avoids collisions. The follower steers so as to avoid collisions and to help the leader carry the object (Panels E- G). Once it is possible the follower drives again in line formation with the leader until the final target position is reached (Panels G- H).

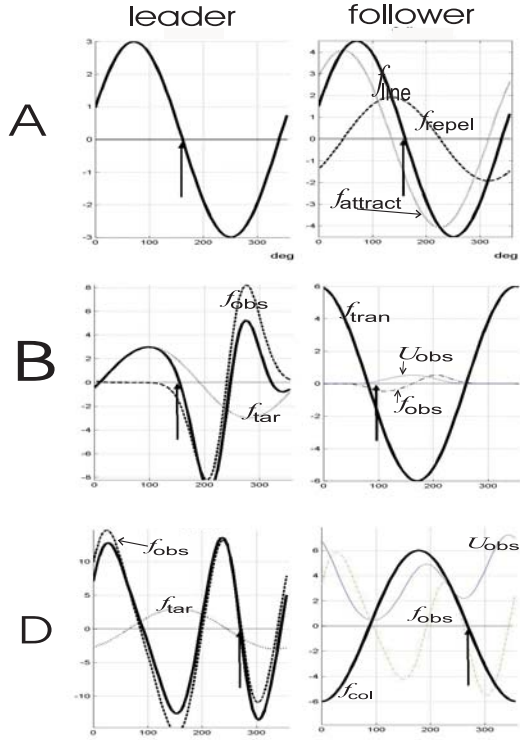


Figure 9: Heading direction dynamics for the two robots when they are at positions depicted in snapshot A, B and D in Figure 8. The black arrow in each plot indicates the current state (i.e. heading direction in the world) of the corresponding robot. As one can see the heading direction of each robot is always very close to a fixed point attractor (i.e. a zero with negative slope) of the resultant dynamics (black bold line). Panel A left plot: Since no obstructions are sensed by the leader its resultant heading direction dynamics (black bold line) is simply the target acquisition dynamics (f_{tar}). Panel A right Plot: since no obstacles are detected by the follower the contributions for its heading direction dynamics are $f_{attract}$ (dotted line) and f_{repel} (dashed line). The resultant dynamics (sum of these contributions) is f_{line} (black bold line). Panel B left plot: Contribution of the sensed obstructions is the dashed line (f_{obs}) and the dotted line represents the contribution of the target (f_{tar}). The resultant dynamics (i.e. sum over all contributions) is the black continuous line. Panel B right Plot: Now also the follower robot senses obstructions (indicated by f_{obs} and U_{obs}). Because the heading direction of this robot is inside the repulsive range (indicated by positive U_{obs} at the value indicated by the arrow, i.e. the current value of follower's heading direction), and the difference between the heading direction of the two robots is larger than 5deg the dynamics is dominated by the term f_{tran} . Panel D left plot: Contribution of the sensed obstructions is the dashed line (f_{obs}) and the dotted line represents the contribution of the target (f_{tar}). The resultant dynamics is the black continuous line. Panel D right Plot: Here the follower robot senses obstructions. Its heading direction is inside the repulsive range (indicated by positive U_{obs}), and the difference between the heading direction of the two robots is smaller than 5deg, thus the resultant dynamics is dominated by the term f_{col} .